Mechanisms of host cell exit by the intracellular bacterium *Chlamydia*

Kevin Hybiske and Richard S. Stephens*

Division of Infectious Diseases, School of Public Health, University of California, Berkeley, CA 94720

Edited by John J. Mekalanos, Harvard Medical School, Boston, MA, and approved May 24, 2007 (received for review April 9, 2007)

The mechanisms that mediate the release of intracellular bacteria from cells are poorly understood, particularly for those that live within a cellular vacuole. The release pathway of the obligate intracellular bacterium *Chlamydia* from cells is unknown. Using a GFP-based approach to visualize chlamydial inclusions within cells by live fluorescence videomicroscopy, we identified that *Chlamydia* release occurred by two mutually exclusive pathways. The first, lysis, consisted of an ordered sequence of membrane permeabilizations: inclusion, nucleus and plasma membrane rupture. Treatment with protease inhibitors abolished inclusion lysis. Intracellular calcium signaling was shown to be important for plasma membrane breakdown. The second release pathway was a packaged release mechanism, called extrusion. This slow process resulted in a pinching of the inclusion, protrusion out of the cell within a cell membrane compartment, and ultimately detachment from the cell. Treatment of *Chlamydia*-infected cells with specific pharmacological inhibitors of cellular factors demonstrated that extrusion required actin polymerization, neuronal Wiskott–Aldrich syndrome protein, myosin II and Rho GTPase. The participation of Rho was unique in that it functioned late in extrusion. The dual nature of release characterized for *Chlamydia* has not been observed as a strategy for intracellular bacteria.

extrusion | lysis | release

Entry and exit are critical steps in the infectious cycles of intracellular pathogens. Although considerable advances have been made in our understanding of the unique strategies used by bacteria to invade cells, an appreciation for exit mechanisms has not been realized. An understanding of the specific pathways of pathogen exit is of fundamental importance to microbial pathogenesis because of its intimate association with dissemination, transmission and inflammation. There is increasing evidence that microbial exit is an organized and directed process mediated by both bacterial and cellular factors. This is best exemplified by *Shigella* and *Listeria*, which promote their escape from phagosomes through the action of pore-forming cytolysins: IpaB for *Shigella* (1), listeriolysin O, and C-type phospholipases for *Listeria* (2, 3). Cellular release then occurs as these bacteria use actin polymerization to protrude out of the cell (4, 5), although additional unknown mechanisms are likely involved (6). In contrast, it has been found that phospholipase activity mediates the release of *R. prowazekii* from phagosomes (7), and a hemolysin is responsible for the phagosomal exit of *T. cruzi* (8).

Intracellular bacteria that reside within a vacuole have the additional challenge of needing to traverse two membranes to successfully escape the host cell. Unfortunately, a limited understanding exists as to how this may be accomplished. One of the better examples is the merozoite-stage rupture of erythrocytes by the malarial parasite *P. falciparum*, in which cysteine proteases have been shown to be essential for sequential rupture of the vacuole and cell (9). Other examples include pore formation-mediated cytolysis by *Legionella* (10) and *Leishmania* (11) and expulsion of *C. neoformans* (12, 13).

Chlamydia is an obligate intracellular bacterium that must overcome these same challenges to complete its infectious cycle. *Chlamydia* spends its intracellular life within a parasitophorous vacuole, or inclusion, a compartment that allows for nutrient acquisition and sequestration from endolysosomal pathways. We are beginning to understand the varied ways in which *Chlamydia* interacts with the host cell to facilitate adhesion, entry, and inclusion biogenesis (14). However, little information exists concerning the mechanisms that mediate the release of *Chlamydia* from either the inclusion or cell. As for most pathogens, it is assumed that *Chlamydia* are released by lysing their host cell (15–20), although it has also been proposed that *Chlamydia* may exit by exocytosis (21) or apoptotic (22) pathways. Deciphering the cellular exit mechanisms of *Chlamydia* will be of fundamental importance to understanding *Chlamydia* pathogenesis, because cellular release directly affects its ability to infect new cells and transmit to new hosts (23).

In this study, a cellular GFP-based approach was used to discern *Chlamydia* exit mechanisms by visualization of chlamydial inclusion dynamics in live cells. *Chlamydia* exit was found to occur by two distinct and independent processes: (*i*) cellular lysis and (*ii*) a packaged release we have called extrusion. Furthermore, essential cellular regulators of each pathway were identified, which enabled independent inhibition and analysis of each exit mechanism.

Results

Visualization of Real-Time Inclusion Dynamics by Fluorescence Microscopy. Our limited understanding of how *Chlamydia* exits cells can be largely attributed to the lack of robust methods for visualizing either the bacteria or the chlamydial inclusion in live cells by fluorescence microscopy. To overcome this limitation, we recognized that the inherent ability of the inclusion to exclude large, soluble fluorescent markers could be used advantageously to visualize it within the cell, analogous to previous observations (24). Accordingly, HeLa cells were transduced with a retrovirus containing the GFP gene. This yielded cells with stable expression of cytosolic GFP that were easily observed live by fluorescence microscopy.

When GFP-HeLa cells were infected with *Chlamydia*, inclusions were visible with live fluorescence microcopy by virtue of their ability to exclude cytosolic GFP. Small inclusions were readily observed in live cells as early as 6 h, and they grew in size to 72 h in accordance with the *Chlamydia* developmental cycle (Fig. 1). Nuclei were also visible by an enrichment of GFP, consistent with previous data (25).

In addition to early and unambiguous visualization of inclusions in living cells, this approach enabled detailed measurement of inclusion dynamics in real-time. Live, *Chlamydia*-infected cells were

Author contributions: K.H. and R.S.S. designed research; K.H. performed research; K.H. contributed new reagents/analytic tools; K.H. and R.S.S. analyzed data; K.H. and R.S.S. wrote the paper.

The authors declare no conflict of interest.

This article is a PNAS Direct Submission.

Abbreviations: N-WASP, neuronal Wiskott–Aldrich syndrome protein; PFO, perfringolysin O.

*To whom correspondence should be addressed. E-mail: rss@berkeley.edu.

This article contains supporting information online at www.pnas.org/cgi/content/full/0703218104/DC1.

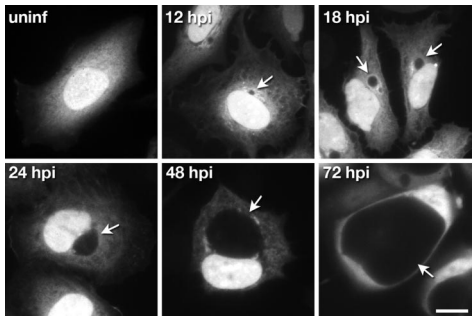

Fig. 1. Detailed visualization of the *Chlamydia* developmental cycle in GFP-HeLa cells. Panels are representative of GFP-HeLa cells infected with *C. trachomatis* L2, and imaged live by confocal microscopy at times indicated. Arrows denote inclusions. (Scale bar: 10 μm.)

subjected to time-lapse fluorescence videomicroscopy, and a 4-h period of chlamydial growth was recorded at 5-min intervals and measured. This allowed the reciprocal spatial relationship between the inclusion and host cytoplasm to be examined. Hallmark differences in inclusion morphology were discerned among different *Chlamydia* species and serovars, analogous to previous descriptions (14, 20).

Inclusions from all chlamydiae exhibited significant dynamic movement, but only at late stages of infection. Late inclusions often were seen to rapidly move inside cells, consistent with previous reports (15, 17, 18). Other typical morphologic events included transient septation of inclusions, displacement of nuclei, and outward blebbing [see examples in supporting information (SI) Movies 1–3]. Interestingly, these phenomena were never observed in early- or mid-stage infected cells (up to 48 h; data not shown). The dynamic and detailed behavior of late-stage inclusions was subsequently used as the basis for identifying the modes of release for *Chlamydia*.

Cellular Exit of *Chlamydia* Is Mediated by Two Distinct Mechanisms. Infected GFP-HeLa cells were examined at 72 h by real-time fluorescence videomicroscopy to identify the general exit pathways used by *Chlamydia*. Analysis of late-stage cellular and inclusion dynamics over 4-h periods of continuous chlamydial growth revealed that *Chlamydia* exit occurred by two mutually exclusive pathways: (*i*) lysis of the inclusion and cell and (*ii*) a packaged release process we have called extrusion. Both release pathways occurred at near equivalent frequencies. Single-cell scoring of *Chlamydia* release pathways from all experiments indicated relative lysis vs. extrusion rates of 47% and 53%, respectively, for *C. trachomatis* L2, 52% and 48% for *C. trachomatis* D, and 68% and 32% for *C. caviae* GPIC. The lesser frequency of extrusion for GPIC-infected cells was likely an underestimate, due to the greater difficulty in discerning inclusion morphology in these cells. Apoptotic phenomena were not observed to participate in chlamydial exit, based on the absence of membrane blebbing, pyknosis, or nuclear fragmentation in infected cells. Apoptotic sequelae were occasionally seen in uninfected cells, consistent with the findings in ref. 26. *Chlamydia* release was found to be independent of host cell type, as similar results were obtained with GFP-MDCK and GFP-Hep2 cells (data not shown).

Lysis Pathway of *Chlamydia* Release. Lysis entailed a spontaneous rupture of both the inclusion and cell. It appeared that lysis was not a consequence of mechanical stress exerted on the cell by the chlamydial inclusion, but rather consisted of an ordered temporal sequence of permeabilizations within the cell. The first step was rupture of the inclusion membrane, identified by the inability of the inclusion to maintain exclusion of cytosolic GFP (Fig. 2 *A–C*, column 2). Subsequently, other intracellular compartments were

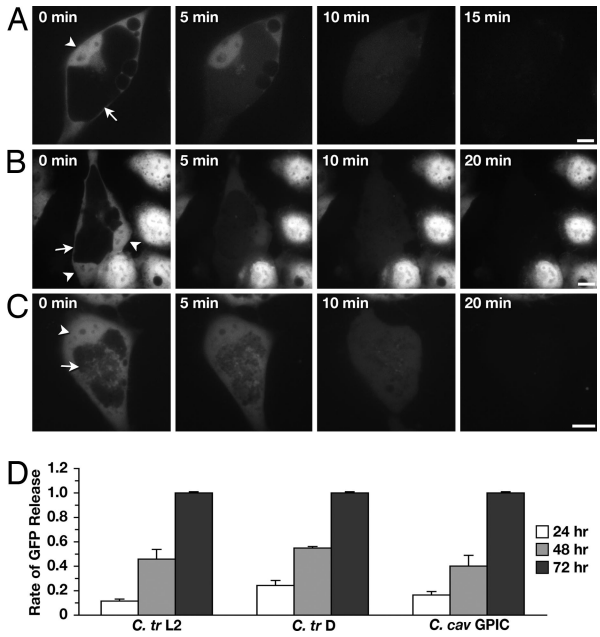

Fig. 2. Lysis mechanism of *Chlamydia* release. GFP-HeLa cells infected with *C. trachomatis* L2 (*A*), *C. trachomatis* D (*B*), and *C. caviae* GPIC (*C*) for 72 h were imaged by live time-lapse videomicroscopy. Representative still frames illustrating the sequence of lysis are shown. Arrows denote inclusions. Arrowheads denote nuclei. (Scale bars: 10 μm.) (*D*) Quantification of lysis by the release of cytosolic GFP into culture supernatants. Fluorometric values are expressed relative to the maximal levels obtained at 72 h. Error bars denote the standard error of the mean ($n = 9$).

permeabilized, demonstrated by the loss of GFP enrichment in nuclei (Fig. 2 *A–C*, column 3). Finally, permeabilization of the plasma membrane completed the pathway, resulting in dispersion of *Chlamydia* elementary bodies and the loss of GFP fluorescence from the cell (Fig. 2 *A–C*, column 4). A representative movie of the lysis pathway is provided (SI Movie 4). Detailed temporal measurements revealed that lysis typically took 16 min for L2, 21 min for D, and 19 min for GPIC.

Another advantage of this GFP-based approach was that the extent and temporal nature of lysis could be quantified in popula-

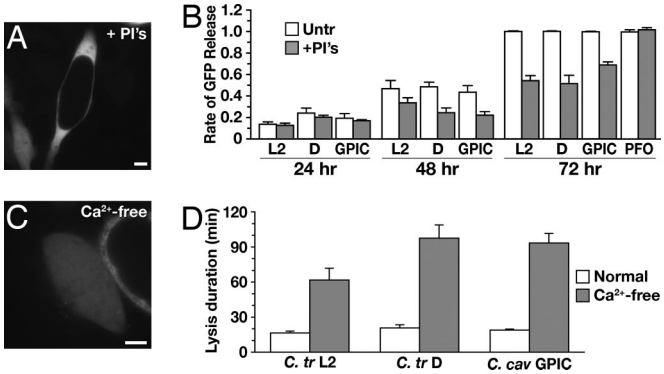

Fig. 3. Lysis is mediated by proteases and intracellular calcium. (*A*) *Chlamydia*-infected GFP-HeLa cells treated with protease inhibitors. (*B*) Quantification of lysis by release of cytosolic GFP in untreated cells (DMSO, white bars) or treated with protease inhibitors (gray bars). Fluorometric values are expressed relative the maximal levels obtained at 72 h. PFO+PI's is expressed relative to untreated (PFO+DMSO) cells. (*C*) *Chlamydia*-infected cell in mid-lysis during Ca^{2+}-free conditions. (*D*) Duration of lysis under normal (white bars) or Ca^{2+}-free (gray bars) conditions. (Scale bars: 10 μm.) Error bars denote the standard error of the mean ($n = 9$).

MICROBIOLOGY

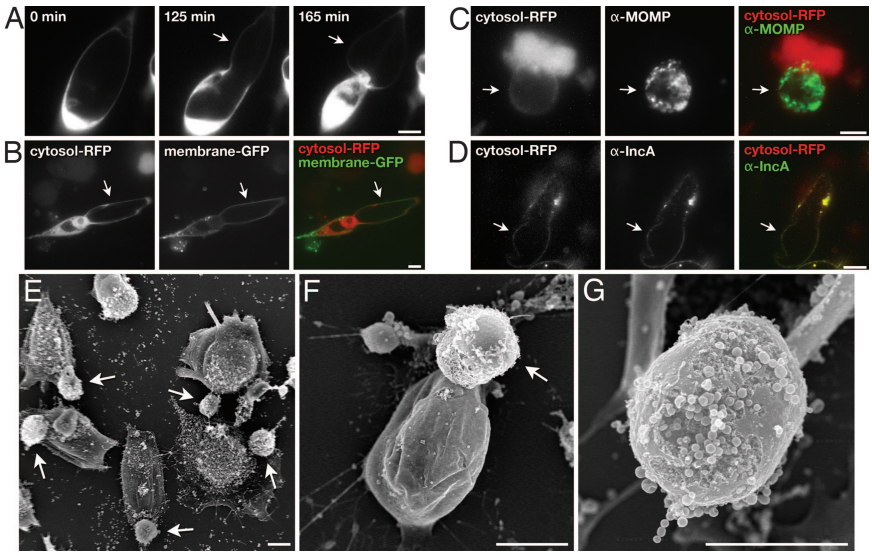

Fig. 4. Extrusion mechanism of *Chlamydia* release. (*A*) Time-lapse videomicroscopy images of extrusion formation. (*B*) Extrusion in cells expressing cytosol-red fluorescent protein and membrane-GFP. Confocal immunofluorescence of extrusions in red fluorescent protein-HeLa cells, using antibodies to MOMP (*C*) and IncA (*D*). (*E*) Scanning EM of a field of cells with extrusions. (*F*) Scanning EM of a single extruded cell. (*G*) Scanning EM of a detached extrusion. Arrows denote extrusions. Minor image enhancements were performed in *A*, *C*, and *D* to improve visualization of extrusions. Enhancements consisted of adjusting brightness and contrast slightly to ensure that the thin cell outlines could be reliably seen by the reader. (Scale bars: 10 μm.)

tions of infected cells by measuring the amount of GFP released into culture supernatants. At 24, 48, and 72 h, cells were rinsed and incubated for 1 h at 37°C. Supernatants were collected, and the extent of lysis during that interval, as indicated by GFP release, was quantified by fluorimetry. In cells infected with *C. trachomatis* L2, a maximal amount of lysis occurred at 72 h (Fig. 2*D*). The amount released at 48 h was 46% of that measured at 72 h, and 11% activity was detected at 24 h. Similar results were obtained with D and GPIC (Fig. 2*D*). Thus, the lysis pathway only occurred at late stages of infection.

Inclusion Lysis Is Mediated by Proteases. The ordered, sequential nature of lysis suggested that it was a biological process and not due to mechanical stress. Possible mechanisms for bacteria-derived membrane permeabilization include cytolysins, phospholipases, and proteases (9, 27). Therefore, we initially tested the potential involvement of cellular or chlamydial proteases in lysis by treating infected cells with protease inhibitors. When *Chlamydia*-infected cells at 72 h were incubated with a mixture of protease inhibitors, lysis was completely inhibited. Remarkably, analysis of live cells by fluorescence videomicroscopy revealed that the initial step of lysis, inclusion rupture, was specifically disrupted (Fig. 3*A*). Significantly, the strongest individual effect occurred with the cysteine protease inhibitor E64, and serine protease inhibitors had no effect (data not shown). Protease inhibitor treatment did not inhibit the morphology or frequency of the extrusion pathway of *Chlamydia* release.

The effect of protease inhibition on lysis was quantified by measuring the release of cytosolic GFP into culture supernatants after 1-h treatments with protease inhibitors. At 72 h, protease inhibitor treatment resulted in significant reductions in lysis [to 54% of untreated levels for L2, 51% for D, and 69% for GPIC (Fig. 3*B*)]. Likewise, the smaller amounts of lysis present at 48 h were also significantly reduced [72% of untreated levels for L2, 50% for D, and 51% for GPIC (Fig. 3*B*)]. Small effects were observed at 24 h. To confirm that the results of protease inhibitor treatment were not due to nonspecific effects on released GFP, we incubated uninfected cells with perfringolysin O (PFO) to perforate cell membranes and elicit GFP release. PFO treatment resulted in GFP release that was roughly 7.5-fold higher than that of *Chlamydia*-infected cells at 72 h; this amount was unaffected by treatment with protease inhibitors (Fig. 3*B*). Thus, protease inhibitors specifically prevented lysis at the step of inclusion rupture, and cysteine proteases were strongly involved.

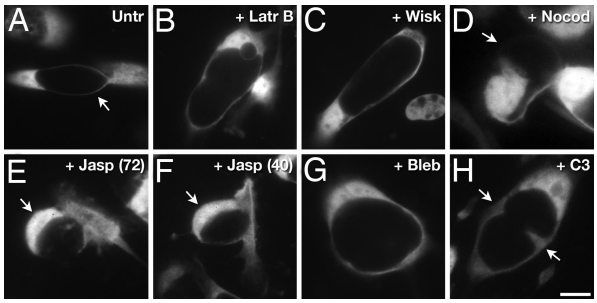

Fig. 5. Extrusion requires actin polymerization by N-WASP, myosin II, and Rho GTPase. Images of *Chlamydia*-infected GFP-HeLa cells untreated (*A*) or treated with Latrunculin B (*B*), Wiskostatin (*C*), Nocodazole (*D*), Jasplakinolide at 72 h (*E*), and Jasplakinolide at 40 h (*F*), Blebbistatin (*G*), and C3 transferase (*H*). Arrows in *A* and *D–F* denote extrusions. Arrows in *H* denote site of pinching. Minor image enhancements were performed in *D–F* to facilitate visualization of extrusions. Enhancements consisted of adjusting brightness and contrast slightly to ensure that the thin cell outlines could be reliably seen by the reader. (Scale bar: 10 μm.)

Calcium-Dependent Permeabilization of Cell Membrane. Because cysteine proteases are often calcium-activated (28), we tested the role of intracellular calcium signaling in the lysis pathway. *Chlamydia*-infected cells at 72 h were preincubated in calcium-free Ringer's solution supplemented with 1,2-bis(2-aminophenoxy)ethane-*N*,*N*,*N*′,*N*′-tetraacetate (BAPTA)-acetoxymethyl ester for 1 h at 37°C to buffer intracellular calcium levels. Cells were maintained in calcium-free solution and the effect on *Chlamydia* release was determined by live fluorescence videomicroscopy. Interestingly, inhibition of calcium signaling significantly impaired the final step of lysis, plasma membrane rupture, with no apparent effect on inclusion rupture (Fig. 3*C* and SI Movie 5). Specifically, a pronounced delay between the onset and conclusion of lysis occurred in calcium-buffered cells. Typically, the entire lysis mechanism took 16 min to complete its course in L2-infected cells, 21 min for *C. trachomatis* D, and 19 min for GPIC (Fig. 3*D*). In calcium-buffered cells, however, lysis was delayed to 62 min for L2, 98 min for D, and 93 min for GPIC (Fig. 3*D*). BAPTA treatment alone (i.e., in calcium-containing extracellular solution) had no effect (data not shown), indicating that the source of calcium influx was from the extracellular solution and not intracellular stores. Thus, the final step in the lysis pathway of *Chlamydia* release was calcium-dependent, and it is possible that proteases were also involved.

Table 1. Frequency of *Chlamydia* release mechanisms after inhibitory treatments

Treatment	Target	Lysis	Extrusion
Untreated (L2)	n/a	0.47 ± 0.06	0.53 ± 0.06
Protease inhibitors	Proteases	0	1.0 ± 0
Ca^{2+}-free + BAPTA-AM	Intracellular calcium	0.52* ± 0.02	0.48 ± 0.02
BAPTA-AM	Intracellular calcium*	0.45 ± 0.05	0.55 ± 0.05
Latrunculin B	Actin polymerization	1.0 ± 0	0
Wiskostatin	N-WASP	1.0 ± 0	0
Nocodazole	Microtubules	0.37 ± 0.03	0.63 ± 0.03
Jasplakinolide	Actin depolymerization	0	1.0 ± 0
Blebbistatin	Myosin II	0.96 ± 0.06	0.04 ± 0.06
C3 transferase	Rho GTPase	0.9 ± 0.1	0.1 ± 0.1

Release mechanisms were scored as lysis or extrusion for at least three separate experiments and a minimum of sixty infected cells. Numerical values represent the frequency of one release pathway relative to each other. Errors denote the standard error of the mean. *, Although lysis was not significantly inhibited, cell membrane rupture was delayed. n/a, not applicable; BAPTA-AM, 1, 2-bis (2-aminophenoxy) ethane-*N*,*N*,*N*′,*N*′ tetraacetate-acetoxymethyl ester.

Extrusion Pathway of *Chlamydia* Release. The second independent *Chlamydia* exit pathway was extrusion, a packaged release process that left the host cell intact. Analysis of inclusion and cellular dynamics by live fluorescence videomicroscopy over 4-h periods of chlamydial growth allowed characterization of the signature events of extrusion: (*i*) protuberance of the membrane-bound inclusion out of the cell, (*ii*) pinching of the inclusion into separable compartments, and (*iii*) presentation of the pinched, protruded inclusion to a tethered location on the cell periphery (Fig. 4*A* and SI Movie 6). The amount of *Chlamydia* packaged within extrusions was variable and ranged from retention of many bacteria within the original, viable cell, to release of the entire chlamydial load. In contrast to the relative rate of lysis, extrusion was slow, typically taking 2–3 h to complete (Fig. 4*A*). Extrusion was similar in cells infected with *C. trachomatis* D or *C. caviae*.

We investigated whether extruded chlamydial inclusions were released out of cells entirely or whether they remained continuous with cells (i.e., surrounded by plasma membrane). HeLa cells were cotransfected with cytosolic-red fluorescent protein and palmitoyl-GFP to label cytoplasm and plasma membranes, respectively. These cells were infected with *Chlamydia* and subjected to live fluorescence videomicroscopy after 72 h. Analysis revealed that extrusions were surrounded by both cytoplasm and plasma membrane (Fig. 4*B*). Furthermore, the absence of a defined membrane barrier between the cell and extrusion suggested that extrusions remained continuous with the cell for >2 h (Fig. 4*B Center*).

Immunofluorescence analysis was performed by using specific antibodies to *Chlamydia*. Staining of the *Chlamydia* outer membrane protein MOMP showed that extrusions contained numerous organisms (Fig. 4*C*). Staining of IncA, an established marker of the chlamydial inclusion (29), demonstrated that extrusion-bound *Chlamydia* remained encased within an intact inclusion membrane (Fig. 4*D*). Importantly, extrusions also contained a thin layer of cytoplasm between plasma and inclusion membranes (Fig. 4 *A–D*). Infected cells were subjected to scanning electron microscopy to determine the morphology and topology of extrusions. At low magnification, extrusion-containing cells were readily abundant (Fig. 4*E*) and extrusions appeared to project in both lateral and upward directions (Fig. 4 *E* and *F*), consistent with fluorescence data. Finally, extrusions were often observed isolated from cells (Fig. 4*G*). Although detached extrusions were usually found intact, an example of a detached extrusion that had fractured open, revealing its dense contents of *Chlamydia*, is shown in Fig. 4*G*.

Extrusion Requires Actin Polymerization, Neuronal Wiskott–Aldrich Syndrome Protein (N-WASP), Myosin II, and Rho GTPase. It seemed likely that the host cytoskeleton was intimately involved with extrusion, given the dramatic morphological changes associated with the pathway. As such, specific inhibitors of cytoskeletal function were used to test for their independent effects on the extrusion mechanism. Late-stage *Chlamydia*-infected GFP-HeLa cells were treated with: latrunculin B, to prevent actin polymerization; nocodazole, to depolymerize microtubules; or wiskostatin, a cell-permeable inhibitor of the actin nucleation factor N-WASP (30). After inhibitor treatment for 1 h at 37°C, cells were subjected to live fluorescence videomicroscopy, and single-cell recordings from 4 h of chlamydial growth were analyzed for effects of drug treatment on extrusion-mediated release. Inhibition of actin and N-WASP completely inhibited extrusion formation (Fig. 5 *B* and *C*, Table 1, and SI Movies 7 and 8) yet had no effect on lysis. In contrast to these results, microtubule disruption had no effect on extrusion or lysis (Fig. 5*D* and Table 1).

A dynamic interplay between actin polymerization and depolymerization are often important for actin-based processes. We directly tested whether actin dynamics were required for extrusion formation or whether stabilized actin filaments were sufficient, by treating *Chlamydia*-infected cells with jasplakinolide, a potent inducer and stabilizer of actin filaments. Remarkably, this treatment induced extrusion formation. After treatment for 30 min at 37°C, nearly all 72-h-infected cells exhibited extrusion when visualized by fluorescence microscopy (Fig. 5*E* and Table 1), and the resulting extrusions were indistinguishable from natural extrusions (example in Fig. 5*A*). Furthermore, application of jasplakinolide to infected cells at 40 h, a time point at which *Chlamydia* release (and extrusion) was minimal, also surprisingly induced extrusions (Fig. 5*F*). Thus, actin depolymerization was not a requirement for extrusion; actin polymerization alone was sufficient to drive the event.

Given the important involvement of actin polymerization in the extrusion pathway, we examined whether actomyosin forces were also required. Treatment of *Chlamydia*-infected cells with blebbistatin, a specific cell-permeable inhibitor of myosin II (31), prevented extrusion formation during time-lapse recordings of live cells (Fig. 5*G*, Table 1, and SI Movie 9). No effect on the frequency or nature of lysis was observed with myosin II inhibition.

The pinching step in the final stage of the extrusion pathway was reminiscent of cytokinesis, and suggested that extrusion might share mechanistic overlap with cytokinesis. Because actin, myosin II, and RhoA are key mediators of contractile ring formation in cytokinesis (32) and the requirements for actin and myosin II in extrusion have already been demonstrated, the additional involvement of Rho GTPase was investigated. *Chlamydia*-infected cells were treated with a cell-permeable derivative of C3 transferase, a potent and specific inhibitor of Rho GTPase. Interestingly, extrusions were arrested at the pinching step, because cells were capable of initial protrusions but unable to complete extrusion (Fig. 5*H*, Table 1, and SI Movie 10).

MICROBIOLOGY

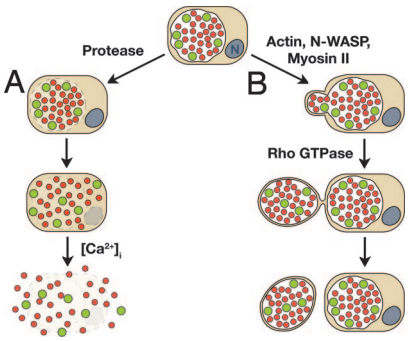

Fig. 6. Dual mechanisms of cellular exit by *Chlamydia*. (*A*) Lysis. (*B*) Extrusion.

Discussion

The GFP-based method described here for visualization of the chlamydial inclusion within live cells holds tremendous promise for the field. This new approach allows for unambiguous analysis of inclusion dynamics throughout the developmental cycle, even as early as 6 h, something that is impossible by light microscopy. This technical advance has enabled us to definitively establish and characterize the two separate cellular release pathways for *Chlamydia* (Fig. 6). Lysis was a destructive mode of release, consisting of sequential rupture of inclusions and cellular membranes; this mode of release was accompanied by death of the host cell. In contrast, extrusion represented a packaged release process in which a portion of the chlamydial inclusion was released by a membranous protrusion. This event left the original cell and residual inclusion intact. Both release pathways occurred at nearly equivalent frequencies. Importantly, the specificity of inhibitors for each release mechanism allowed for their independent examination, and supported the proposal that lysis and extrusion are mutually exclusive pathways.

Our findings suggest that lysis and extrusion are prevalent among the different chlamydiae. No fundamental differences in molecular mechanisms were observed among the organisms used in this study, despite gross differences in inclusion morphology. The relative frequencies of lysis and extrusion were tightly conserved for *C. trachomatis*. Extrusion was less common in cells infected with *C. caviae*, although this is partly attributable to the greater difficulty in visualizing these inclusions. Both release pathways occurred only late in the developmental cycle for all chlamydiae. Finally, these mechanisms were independent of host cell type. Identical results to those described, using HeLa cells, were obtained with Hep2 and polarized MDCK epithelial cells.

The breadth and scope of these results are strengthened by previous findings. Lysis of *Chlamydia*-infected cells is a general phenomenon that has been experimentally observed (15–20), although its mechanisms were previously unknown. Interestingly, pseudopod-like extensions on *Chlamydia*-infected cells have been briefly described for different *Chlamydia* species, cells and tissues (15–17). Focal elongation of inclusions has also been observed, although this event was consequent with rupture of cells (33). It is thus unclear whether these observations are related to the extrusion mechanism characterized in the present study. If so, it reinforces the hypothesis that extrusion is a pervasive cellular release pathway for *Chlamydia*. In addition, observed release of *C. trachomatis* D was proposed to occur by an exocytic-like mechanism that left host cells intact (21). Although both studies demonstrate viable cells after *Chlamydia* release, they differ in that we found no evidence of membrane fusion, an event that would have been efficiently detected by our method.

The existence of two drastically different cellular release pathways for *Chlamydia*, coupled with evidence that they may also occur *in vivo* (16), has profound implications for *Chlamydia* infections. First, they imply that differential means of dissemination by newly formed *Chlamydia* elementary bodies are possible. Upon release by lysis, individual bacteria are expected to diffuse outward and infect new cells. The consequence of extrusion-mediated release is less clear, although the implication is that *Chlamydia* can disseminate via a host cell membranous, protected compartment. Although the molecular mechanisms of scission remain unknown, it was evident that extrusions eventually detach from cells, based on EM data and the presence of residual small inclusions. This mechanism of dissemination could offer protective benefits to *Chlamydia*. Extrusion-bound bacteria might be shielded from preexisting local immune responses; subsequent rupture and release of free organisms might occur only after they have moved to a safer location. Alternatively, extrusions could be engulfed by macrophages, thereby facilitating secondary infection and dissemination in the host.

The inherent ability of extrusion to shed away infectious *Chlamydia* elementary bodies while leaving behind a viable infected cell provides tantalizing evidence, although speculative, for a cellular persistence mechanism. Persistence is a key concept in *Chlamydia* pathogenesis and describes the ability of *Chlamydia* to avoid elimination within the host and thus cause chronic infections (34). Unfortunately, evidence for exactly how this occurs at the cellular level is lacking. Extrusion provides a possible framework for how persistence may be achieved by *Chlamydia* residing within a host cell for an extended time. A recent report that described the existence of small primary inclusions at late stages of infection lends further credence to this idea (35). However, further work must be done to ascertain how viable post-extrusion cells are and how the *Chlamydia* developmental cycle proceeds in residual inclusions.

An important unanswered question concerns the signals that initiate and dictate one release pathway over the other. The concept that initiating signals for *Chlamydia* release may come from the bacteria is supported by a number of arguments. First, the morphological events that characterized *Chlamydia* release were never detected in uninfected cells. Second, lysis had an unambiguous inside-out (inclusion–cytosol–plasma membrane) spatial and temporal nature that originated from the inclusion. Third, both mechanisms were observed in cells that harbored moderate-sized inclusions. Thus, *Chlamydia* release was likely a consequence of a biological interaction between the inclusion and cell established late in the developmental cycle and was not due to physical stress imposed on the cell simply by a massive inclusion. Recent evidence that chlamydial proteins, including a protease, accumulate in the cytoplasm of cells in a temporal manner support this possibility (36–39). In addition, very late (30 h after infection) gene expression patterns have been reported (40), thus supporting the view that a late-expressed chlamydial protein could induce release.

The strategies used by intracellular bacteria to escape cells are in general poorly understood. This study establishes a dual-mechanism strategy for cellular exit by *Chlamydia* that may be used by other organisms. Our data are consistent with the proposal that cell lysis is a pervasive escape mechanism (9–11). The temporal nature of *Chlamydia*-induced lysis and its regulation by cysteine proteases is analogous to what has been described for the exit of *P. falciparum* from erythrocytes (9). Given the disparity between organisms, this important similarity suggests that protease-mediated membrane lysis might be a fundamental strategy used by intracellular pathogens. In contrast, the extrusion phenomenon characterized for *Chlamydia* represents an unusual escape mechanism for intracellular bacteria. Moreover, the involvement of actin polymerization in extrusion represents a previously undescribed mechanism of host–pathogen interaction.

Materials and Methods

Reagents. Unless otherwise specified, all reagents and chemicals were obtained from Sigma (St. Louis, MO). Additional reagents and concentrations used include latrunculin B (500 nM) and

jasplakinolide (1 μM) (Molecular Probes, Eugene, OR); nocodazole (30 μM), wiskostatin (50 μM) and blebbistatin (50 μM) (Calbiochem, San Diego, CA); and cell permeable C3 transferase (2.5 μg/ml) (Cytoskeleton, Denver, CO). The protease inhibitor mixture consisted of (10 μg/ml) antipain, leupeptin, pepstatin A, chymostatin, and 1 μM E64.

Cell Culture and Infections. *C. trachomatis* serovars L2 or D, and *C. caviae* GPIC were grown and elementary bodies were purified as described in ref. 41. HeLa 229 cells were plated on glass bottom culture dishes (MatTek, Ashland, MA) or 24-well plates and typically infected with *Chlamydia* diluted in Hanks's balanced salt solution (HBSS) at a multiplicity of infection ≤ 1, for 1.5 h at 25°C (L2) or with centrifugation at 600 $\times$ *g* (D and GPIC). Cells were washed with HBSS and incubated in normal growth media at 37°C for times indicated.

To neutralize intracellular calcium signaling, infected cells were washed and incubated for 1 h in calcium-free ringers solution (42) (155 mM NaCl/4.5 mM KCl/3 mM $MgCl_2$/10 mM D-glucose/5 mM Hepes, pH 7.4) plus 50 μM 1,2-bis(2-aminophenoxy)ethane-*N*,*N*,*N*′,*N*′-tetraacetate-acetoxymethyl ester (BAPTA-AM). After BAPTA-AM treatment, cells were washed and incubated in calcium-free ringers solution. For videomicroscopy experiments, Hepes was increased to 10 mM to maintain neutral pH while in CO_2-free conditions.

Generation of GFP-HeLa Cells. HeLa cells with stable expression of cytosolic GFP were generated by transduction with a retrovirus containing the GFP gene (pLEGFP-N1; Clontech, Mountain View, CA). Positive transformants were selected with 500 mg/ml neomycin (Invitrogen, Carlsbad, CA) and propagated.

Expression of cytosol-red fluorescent protein and palmitoyl-GFP in HeLa cells was accomplished by DNA transfection (Effectene; Qiagen, Valencia, CA) with 0.5 μg of DsRed-Express (Clontech) and 0.5 μg palmitoyl-GFP [generously provided by T. Machen (University of California, Berkeley)].

Fluorescence Videomicroscopy. Infected GFP-HeLa cells were washed with HBSS and immersed in HBSS plus 10 mM Hepes. Cells were placed in a 37°C thermistor-controlled heated stage (Warner Instruments, Hamden, CT) mounted on a Nikon (Tokyo, Japan) inverted microscope equipped with a QLC100 real-time spinning disk confocal system (VisiTech, Sunderland, U.K.) and a $\times$60 oil objective (N.A. = 1.4). Images were acquired at 5-min intervals, using QED*InVivo* software (MediaCybernetics, Silver Spring, MD). Movies were compiled with QuickTime Pro on a Macintosh G5 (Apple, Cupertino, CA). Recordings and images are representative of at least three separate experiments.

Quantification of GFP Release. Infected GFP-HeLa cells were rinsed and pulsed with clean HBSS (plus protease inhibitors or DMSO) for 1 h at 37°C. Supernatants of cultures were collected and cleared of debris by microcentrifugation (100 $\times$ *g* for 4 min). Samples were analyzed for raw fluorescence, using a 20/20^n Luminometer with a 475- to 545-nm excitation emission fluorescent module (Turner BioSystems, Sunnyvale, CA). HBSS alone was measured for background fluorescence.

For PFO-mediated GFP release, cells were chilled on ice for 15 min and subsequently incubated with recombinant PFO [a gift from D. Portnoy (University of California, Berkeley)] diluted in HBSS for 10 min on ice. Unbound toxin was removed by rinsing and cells were incubated in HBSS for 1 h at 37°C to allow release of cytosolic GFP.

Immunofluorescence. Cells were washed with PBS and fixed with 3.7% formaldehyde/PBS for 10 min, permeabilized with 0.5% Triton X-100/PBS for 15 min, and blocked with 1% BSA/PBS for 20 min, all at 25°C. Cells were incubated for 1 h at 25°C with primary antibodies to either MOMP (43), IncA [a gift from D. Rockey (Oregon State University, Corvallis, OR)] or Alexa-488-GFP (Molecular Probes), and for 45 min with secondary antibody, Alexa-488 or Alexa-594 (Molecular Probes). Images were acquired by using the microscope setup described in *Fluorescence Videomicroscopy*. Minor enhancements were performed by using Photoshop (Adobe, San Jose, CA).

Electron Microscopy. Cells were fixed in 2% glutaraldehyde for 2 h, washed with cacodylate buffer (pH 7.2), and submitted to the University of California Electron Microscopy Laboratory for further processing and coating. Preparations were examined with a Hitachi (Yokohama, Japan) S-5000 scanning electron microscope.

We thank Profs. T. Machen and J. Forte (University of California, Berkeley) for support, D. Portnoy (University of California, Berkeley) for recombinant PFO, and D. Rockey (Oregon State University, Corvallis, OR) for antibodies to IncA. We thank G. Min and the staff of the University of California Berkeley Electron Microscope Laboratory for guidance and support. We also thank P. S. Hefty (University of Kansas, Lawrence, KS) for careful review of the manuscript. This work was supported by National Institutes of Health Grants HL071730 and AI042156.

1. High N, Mounier J, Prevost MC, Sansonetti PJ (1992) *EMBO J* 11:1991–1999.
2. Gaillard JL, Berche P, Mounier J, Richard S, Sansonetti P (1987) *Infect Immun* 55:2822–2829.
3. Smith GA, Marquis H, Jones S, Johnston NC, Portnoy DA, Goldfine H (1995) *Infect Immun* 63:4231–4237.
4. Sansonetti PJ, Mounier J, Prevost MC, Mege RM (1994) *Cell* 76:829–839.
5. Tilney LG, Portnoy DA (1989) *J Cell Biol* 109:1597–1608.
6. Theriot JA (1995) *Annu Rev Cell Dev Biol* 11:213–239.
7. Winkler HH, Daugherty RM (1989) *Infect Immun* 57:36–40.
8. Andrews NW (1990) *Exp Parasitol* 71:241–244.
9. Rosenthal PJ (2004) *Int J Parasitol* 34:1489–1499.
10. Alli OA, Gao LY, Pedersen LL, Zink S, Radulic M, Doric M, Abu Kwaik Y (2000) *Infect Immun* 68:6431–6440.
11. Noronha FS, Cruz JS, Beirao PS, Horta MF (2000) *Infect Immun* 68:4578–4584.
12. Ma H, Croudace JE, Lammas DA, May RC (2006) *Curr Biol* 16:2156–2160.
13. Alvarez M, Casadevall A (2006) *Curr Biol* 16:2161–2165.
14. Hackstadt T (1999) in *Chlamydia: Intracellular Biology, Pathogenesis, and Immunity*, ed Stephens RS (Am Soc Microbiol, Washington, DC), pp 101–138.
15. Campbell S, Richmond SJ, Yates P (1989) *J Gen Microbiol* 135:1153–1165.
16. Doughri AM, Storz J, Altera KP (1972) *J Infect Dis* 126:652–657.
17. Neeper ID, Patton DL, Kuo CC (1990) *Infect Immun* 58:2042–2047.
18. Patton DL, Chan KY, Kuo CC, Cosgrove YT, Langley L (1988) *Invest Ophthalmol Vis Sci* 29:1087–1095.
19. Todd WJ, Storz J (1975) *Infect Immun* 12:638–646.
20. Rockey DD, Fischer ER, Hackstadt T (1996) *Infect Immun* 64:4269–4278.
21. Todd WJ, Caldwell HD (1985) *J Infect Dis* 151:1037–1044.
22. Perfettini JL, Hospital V, Stahl L, Jungas T, Verbeke P, Ojcius DM (2003) *Biochimie* 85:763–769.
23. Schachter J (1999) in *Chlamydia: Intracellular Biology, Pathogenesis, and Immunity*, ed Stephens RS (ASM, Washington, DC), pp 139–169.
24. Grieshaber S, Swanson JA, Hackstadt T (2002) *Cell Microbiol* 4:273–283.
25. Llopis J, McCaffery JM, Miyawaki A, Farquhar MG, Tsien RY (1998) *Proc Natl Acad Sci USA* 95:6803–6808.
26. Zhong Y, Weininger M, Pirbhai M, Dong F, Zhong G (2006) *J Infect* 53:408–414.
27. Goebel W, Kreft J (1997) *Trends Microbiol* 5:86–88.
28. Yamashima T (2004) *Cell Calcium* 36:285–293.
29. Rockey DD, Heinzen RA, Hackstadt T (1995) *Mol Microbiol* 15:617–626.
30. Peterson JR, Bickford LC, Morgan D, Kim AS, Ouerfelli O, Kirschner MW, Rosen MK (2004) *Nat Struct Mol Biol* 11:747–755.
31. Straight AF, Cheung A, Limouze J, Chen I, Westwood NJ, Sellers JR, Mitchison TJ (2003) *Science* 299:1743–1747.
32. Glotzer M (2005) *Science* 307:1735–1739.
33. de la Maza LM, Peterson EM (1982) *Exp Mol Pathol* 36:217–226.
34. Hogan RJ, Mathews SA, Mukhopadhyay S, Summersgill JT, Timms P (2004) *Infect Immun* 72:1843–1855.
35. Beatty WL (2007) *Cell Microbiol*, 10.1111/j.1462–5822.2007.00945.x.
36. Clifton DR, Fields KA, Grieshaber SS, Dooley CA, Fischer ER, Mead DJ, Carabeo RA, Hackstadt T (2004) *Proc Natl Acad Sci USA* 101:10166–10171.
37. Fields KA, Hackstadt T (2000) *Mol Microbiol* 38:1048–1060.
38. Subtil A, Delevoye C, Balana ME, Tastevin L, Perrinet S, Dautry-Varsat A (2005) *Mol Microbiol* 56:1636–1647.
39. Zhong G, Fan P, Ji H, Dong F, Huang Y (2001) *J Exp Med* 193:935–942.
40. Nicholson TL, Olinger L, Chong K, Schoolnik G, Stephens RS (2003) *J Bacteriol* 185:3179–3189.
41. Koehler JE, Burgess RR, Thompson NE, Stephens RS (1990) *J Biol Chem* 265:13206–13214.
42. Fomina AF, Fanger CM, Kozak JA, Cahalan MD (2000) *J Cell Biol* 150:1435–1444.
43. Stephens RS, Tam MR, Kuo CC, Nowinski RC (1982) *J Immunol* 128:1083–1089.

MICROBIOLOGY